HHS Public Access

Author manuscript

Oncogene. Author manuscript; available in PMC 2017 September 12.

Published in final edited form as:

Oncogene. 2017 January 12; 36(2): 168–181. doi:10.1038/onc.2016.197.

Elevated STAT3 expression in ovarian cancer ascites promotes invasion and metastasis: a potential therapeutic target

Uksha Saini[#1], **Shan Naidu**[#1], **Adam C. ElNaggar**[1], **Hemant Kumar Bid**[1], **John J. Wallbillich**[1], **Kristin Bixel**[1], **Chelsea Bolyard**[2], **Adrian A. Suarez**[1], **Balveen Kaur**[2], **Periannan Kuppusamy**[3], **John Hays**[1], **Paul J. Goodfellow**[1], **David E. Cohn**[1,#], and **Karuppaiyah Selvendiran**[1,#]

[1]Division of Gynecologic Oncology, Comprehensive Cancer Center, The Ohio State University Wexner Medical Center, Columbus, OH

[2]Department of Neurological Surgery, The Ohio State University, Columbus, OH

[3]Department of Radiology, Dartmouth Medical School, Hanover, NH

[#] These authors contributed equally to this work.

Abstract

Although activation of the STAT3 pathway has been associated with tumor progression in a wide variety of cancer types (including ovarian cancer), the precise mechanism of invasion and metastasis due to STAT3 are not fully delineated in ovarian cancer. We found that pSTAT3 Tyr705 is constitutively activated in patient ascites and ascites-derived ovarian cancer cells (ADOCCs), and the range of STAT3 expression could be very high to low. In vivo transplantation of ADOCCs with high pSTAT3 expression into the ovarian bursa of mice resulted in a large primary tumor and widespread peritoneal metastases as well liver. In contrast, ADOCCs with low STAT3 expression or ADOCCs with STAT3 expression knocked down led to reduced tumor growth and an absence of metastases *in vivo*. Cytokines derived from the ADOCC culture medium activate the IL-6/STAT pathway in the STAT3 knockout (*Ko)* cells, compensating for the absence of inherent STAT3 in the cells. Treatment with HO-3867 (a novel STAT3 inhibitor at 100 ppm in an orthotopic murine model) significantly suppressed ovarian tumor growth, angiogenesis, and metastasis by targeting STAT3 and its downstream proteins. HO-3867 was found to have cytotoxic effects in *ex-vivo* cultures of freshly-collected human ovarian cancers, including those resistant to platinum-based chemotherapy. Our results show that STAT3 is necessary for ovarian tumor progression/metastasis

[#]Corresponding Authors: Karuppaiyah Selvendiran, Ph.D, Assistant Professor, Division of Gynecologic Oncology, The Ohio State University Wexner Medical Center, Columbus, OH 43210. Phone: 614-685-6574, selvendiran.karuppaiyah@osumc.edu or David Cohn, MD, Director Division of Gynecologic Oncology, Stuart M. Sloan – Larry J. Copeland MD Chair, Professor of Obstetrics & Gynecologic, The Ohio State University Wexner Medical Center, Columbus, OH -43210, david.cohn@osumc.edu.

CONFLICT OF INTEREST: The authors declare no conflict of interest.

Author Contributions K.S., and D.E.C. designed all experiments. U.S., and S.N, performed the majority of the in vivo efficacy experiment assays and analyzed the data collected. S.N. U.S. and A.A.S. performed all the in vivo tumor, histopathology, and imaging work. S.N., U.S. and A.C.E. performed the primary *ex vivo* assays. J.J.W., A.C.E., and K.B. assisted in collecting ascites from human subjects. H.K.B., C.B., and B.K. helped to conduct the kinase, angiogenesis and luciferase assays. P.K. were responsible for the synthesis of the DAP compounds as well as the chemical characterization and analyses. U.S, J.J.W., K.S. and D.E.C. wrote, edited, and proofread the manuscript.

and highlight the potential for targeting STAT3 by HO-3867 as a therapeutic strategy for ovarian cancer.

Keywords

STAT3; Ovarian cancer; Ascites; orthotopic tumor; HO-3867; *Ex-vivo*

Introduction

Ovarian cancer is the most lethal gynecologic malignancy and fifth overall in terms of female cancer deaths in the United States[1, 2]. Metastasis is the major factor governing patient survival and accounts for 80 to 90 % of all ovarian cancer deaths[3, 4, 5]. Thus, the control of ovarian cancer metastasis is the ultimate challenge in saving lives of patients diagnosed with ovarian cancer, as metastasized disease is often referred to as a situation in which “the horse has left the barn”. The presence of ascites has been directly correlated to the peritoneal spread of ovarian cancer[6, 7, 8]. While the combination of these two factors is associated with a poor prognosis the expression of oncogenic proteins and growth factors in ascites and their effects on the ovarian tumor metastatic microenvironment remain poorly understood. Among these factors, the STAT3 oncogene is of particular interest to our group as we have found constitutive expression of pSTAT3 Tyr705 in ovarian cancer patient ascites.

Activation of STAT3 is known to contribute to the aggressiveness of ovarian cancer, promoting cellular proliferation as well as the resistance to chemotherapeutic drugs[9, 10]. However, the exact role of pSTAT3 expression levels in ovarian cancer patient ascites, invasion and metastasis is not yet well defined using a relevant, pre-clinical tumor model. In this study, we used STAT3 knock down/over expression models to show that STAT3 is necessary for ovarian tumor progression and metastasis. We also used an orthotopic ovarian tumor growth and metastasis model to demonstrate the selectively cytotoxic potential of HO-3867, our novel STAT3 inhibitor. We have previously developed, and reported, a novel class of diarylidenyl-piperidone (DAP, HO-3867) based, bi-functional compounds capable of selectively targeting STAT3[11, 12, 13] and inhibiting ovarian tumor growth in a xenograph model[14, 15, 16]. Synthetic small molecules, natural compound analogues, and synthetic peptides have been used to develop an inhibitor of STAT3 capable of decreasing STAT3 expression and inhibiting tumor growth[17]. Curcumin analogues (LLL12 and FLLL32), and synthetic peptides (APT-125) have been evaluated for their ability to inhibit STAT3 activity *in vitro* and antitumor efficacy *in vivo* in a xenograft model[18, 19, 20, 21]. However, the efficacy of those STAT3 inhibitors have not been confirmed with a pre-clinical model (such as orthotopic ovarian tumor) or in an ex vivo drug testing model.

This is the first study to show that STAT3 is necessary for ovarian tumor progression/metastasis and that pSTAT3 Tyr705 is highly expressed in ascites fluid obtained from patients with ovarian cancer. We also report on the unique activity of the STAT3 inhibitor HO-3867 against ovarian cancer. Previously, no commercially available STAT3 inhibitor has shown efficacy using an orthotopic tumor model. In addition, most small molecule STAT3

inhibitors do not reach their target sites. However, in this study we report a novel, orthotopic mouse model, as well as an ex-vivo tissue culture, showing efficacy of HO-3867, against ovarian cancer. Further, we note a higher accumulation of HO-3867 in ovarian tumor tissues. Our results highlight the role of STAT3 in ovarian tumor growth and metastasis as well as the therapeutic potential of targeting STAT3 by HO-3867 using a relevant orthotopic mouse model.

RESULTS

Isolation and characterization of ascites derived cancer cells

We collected the ascites fluid from 20 different patients with high-grade serous ovarian cancer patients after signed consent. The ascites derived ovarian cancer cells (ADOCCs) attached to the bottom of the plates in the first 12 hours and the cells were allowed to multiply thereafter. The ADOCCs (A195) displayed a typical cobblestone appearance under the light microscope (Fig.1A). The ADOCCs were confirmed for their epithelial origin by immunocytochemistry (ICC) using Pan cytokeratin; 99% of the cells were pan CK positive (Fig. 1B, **representative for A195**). We then evaluated the cells for pSTAT3 expression, 90–95% of the cells displayed accumulation of pSTAT3 Tyr705 (Fig.1C and D). The localization of pSTAT3 705 varies widely in different cells like predominantly cytoplasmic in ADOCC (Fig. 1C) and nuclear in TR127 (Fig. 1D). Additional (ICC) confirmation of ascites from multiple patients is shown in Suppl. Fig. S1A. On Western Blot analysis of protein expression by ADOCCs, pSTAT3 Tyr705 was constitutively expressed in a majority of samples, while pSTAT3 Ser727 was not (Fig.1E). Out of the 20 different patient ascites collected and analyzed, 18 had high pSTAT3 expression. ELISA array analyses of total STAT3 and pSTAT3 on ascites, primary tissue and metastatic sites also confirmed this variable pattern of expression. Levels of total STAT3 and pSTAT3 expression in metastatic sites were higher than in the primary tumor sites of ovary (Fig.1F& Sup. Fig.S1B). mRNA expression was analyzed using real time quantitative PCR for STAT3, and it target genes of cyclin D1, cyclin D2, VEGF, IL6 and VEGFR2, relative expression levels of ascites from different patients in Sup. Fig. S1C. The exception was sample A263, which showed no pSTAT3 Tyr705 expression, in contrast, the highest pSTAT3 Tyr705 expression was noted in sample A352. The samples with the lowest (A263) and highest (A352) levels of pSTAT3 expression were each further evaluated with a migration assay and an analysis of expression of pSTAT3 target genes. A352 exhibited a much higher rate of cell migration, relative expression of c-MYC, VEGF, MMP-2,9, and surviving tendency compared to A263 (Fig. 1G&H). Taken together, these findings suggest that increased STAT3 expression renders a kind of migration advantage to the ascites, which may assist in the spread of disease to other organs. To further evaluate these findings *in vivo*, we injected ADOCCs with the highest and lowest STAT3 expression, respectively, into mouse ovaries. Since the ADOCCs could not be cultured beyond passage 3, we created a STAT3 overexpression (OE) construct using the A2780 ovarian cancer cell line, which was confirmed by western blot (Fig. 1I). The OE cells, when injected in mice, displayed a very large ovarian tumor as well as distant metastases invading the mesentery, peritoneum and the liver (Fig.1J); implying that constitutive expression of STAT3 is involved in ovarian tumor migration and metastasis. The tumor weight was significantly higher in STAT3 OE transplanted mice compare with wt type

tumor (Fig.1K). When we checked the pSTAT3 705 expression level in the tissues from organs collected from the STAT3 OE and A2780 Wt mice, we found that a consistent high level of pSTAT3 705 was maintained in the primary ovarian tumor as well as the metastasized sites in the former case but not so much in the latter case (Sup.Fig.1D). The STAT3 OE construct, hence provides the initial `kick' to the STAT3 expression, which continues to self-sustain itself through the life time of the mouse.

Effect of shRNA STAT3 knockdown in ovarian cancer

Although *in vitro* studies have shown that knocking down STAT3 by shRNA inhibits the growth of the CAOV3 ovarian cancer cell line[22], still there is no clear evidence on the role of STAT3 in tumor growth and metastasis. Therefore, it would be interesting to observe the effect of knockdown of STAT3 on cell/tumor growth and migration/invasion behavior. We used a shRNA approach for STAT3 knockdown in A2780R cells, which was confirmed by Western Blot (Fig. 2A). Cell growth assays of the knockdown cells showed a growth decline within the first 24 hours when compared to the wild type (Wt) (Fig. 2B); the trend continued up to 48 hours. Since the *Ko* displayed less vigorous growth in culture, we hypothesized that there might also be changes in the wound closure and invasion behaviors of the cells. To confirm this, we performed a wound healing assay, where a monolayer of cells growing on a petri dish were scratched uniformly and observed at 24 hours for their ability to repair the damaged area. The *Ko* cells migrated to approximately 50% of the wounded area while the Wt cells migrated into 95% of the area (Fig. 2C). The cell invasion assay, which measures the number of cells traversing a porous membrane, also revealed blocked invasion of cells for *Ko* as compared to the Wt cells (Fig. 2D & E). This was further confirmed at the mRNA level using real time quantitative PCR to check the relative expression of genes related to angiogenesis, cell survival and cell proliferation. The *Ko* showed decreased STAT3 (6-fold), VEGF (8.4-fold), cyclin D2 (1.5-fold), Akt (1.6fold), cmyc (3-fold), ATF2 (3.6-fold) and survivin (2-fold) (Fig. 2F). Taken together, these results suggest that deleting STAT3 inhibits the expression of a number of genes responsible for cell survival, migration and invasion. These findings were further evaluated in vivo. The Wt and *Ko* cells were injected into the right ovarian bursal cavity of nude mice (Sup. Figs. S2A&B). Tumor mass was decreased in the mice injected with the *Ko* cells (Fig.2G). The measured tumor weight for the *Ko* was 5 times less than that for the Wt (Fig.2H). These results add support to the role of STAT3 in tumor progression and its ability to regulate the expression of different genes.

STAT3 in supernatant from ADOCCs is responsible for reinstating `virulence' in the knockdown cells

When it became apparent that STAT3 plays an important role in ovarian cancer progression and metastasis, we wished to better understand whether this STAT3-mediated “virulence factor” was inside or outside of the cells. To investigate this, we collected the medium used to culture ADOCCs (conditioned medium) and treated the A2780 Wt and *Ko* cells with this medium. Wound healing assays showed that the addition of supernatant restores the migration capability in the knockdown cells and it was observed that 75–80% of the gap was filled within the first 24 hours (Fig.3A). The invasion assay also confirmed the same (Fig. 3B). The fact that the conditioned medium enabled the *Ko* cells to regain their diminished migration capacity, we thought that it was imperative to analyze the cytokine composition of

the conditioned medium. This was done using multi analyze cytokine ELISA array for simultaneous detection of 12 cytokines like IL1α, IL1β, IL2, IL4, IL5, IL6, IL8, IL10, IL12, IL13, IL17A, GM-CSF. The conditioned medium displayed a very high level of IL6 and IL8 (Fig. 3C &D) which proves that in the absence of constitutive activation of STAT3 (as in STAT3 *Ko*), cytokines induce the endogenous STAT3 transcriptional activity. These findings suggest a critical role for STAT3 not just in promoting growth but also in bestowing tumor cells with aggressive phenotypic features. When injected into mice, both Wt and *Ko* cells pretreated with conditioned medium (CM) induced significantly larger tumors in the ovaries but the CM-treated *Ko* cells showed metastases to the mesentery as well (Fig.3E), mimicking the clinical disease process observed in patients with ovarian cancer. A comparison of the relative expression levels of mRNA of the harvested tissues (primary ovarian cancer tissue as well as the metastasized sites) revealed a higher expression of STAT3, CK19, CK20, cyc D1, cyc D2, MMP9 and VEGF as compared to the primary ovarian cancer tissue (Fig. 3F). Our above research findings are indicated that targeting STAT3 using a orthotopic ovarian tumor model and evaluate therapeutic efficacy of STAT3 inhibitors on the primary ovarian tumor, and assess the potential for treatment of metastatic disease.

Effect of HO-3867 on orthotopic ovarian tumor using established and primary ovarian cancer cell population

We used an established ovarian cancer cell line (SKOV3) and a primary ascites-derived ovarian cancer cell line (TR-127) for injection into the ovarian bursa of mice. The orthotopic mouse model was developed to resemble human ovarian cancer and provide relevant insight into treatment strategies. Tumor implants were monitored by MRI for tumor growth and progression. We used a HO-3867, a novel STAT3 inhibitor developed by our lab, to treat the ADOCC and SKOV3 orthotopic ovarian cancer model. Based on previous work from our lab[14], 50 and 100ppm doses were administered orally to the tumor-bearing mice. As platinum-containing agents are a mainstay of ovarian cancer treatment, we compared cisplatin (CP 4mg/kg, intraperitoneally (IP) twice weekly), with HO-3867. Figure 4A shows in vivo MRI imaging of the control tumor (untreated) and treated tumor mice. As is evident from the coronal plane image, the tumor size is smallest for the mice treated with HO-3867 and cisplatin (CP). A reduction in tumor mass was evident in both CP and HO-3867 treatments (Fig. 4B, 4C and Sup. Fig. S3A–C). There was no significant difference between CP and HO-3867 at 100ppm and both treatments demonstrated significantly decreased tumor mass compared to HO-3867 at 50ppm. Similar results were observed when TR-127 cells transplanted into the orthotopic mouse model were treated with HO-3867 (Fig. 4D&E). Untreated mice also had a large amount of ascites compared to the HO-3867 treated mice (mean 900μl vs 75μl $p \leq 0.0005$, Fig. 4F). We also measured the bio-availability of HO-3867 in multiple organs in the orthotopic mouse model. Tissues from ovaries, kidneys, and livers from control (untreated) and HO-3867-treated mice were collected and prepared for EPR analysis as described previously[23]. A substantial amount of HO-3867 was detected in the ovarian tumor, kidney and liver tissues using EPR spectroscopy (Fig. 4G and Sup. Fig. S3D). In addition, HO-3867 and its chief metabolites were confirmed using liquid chromatography mass spectroscopy (LCMS) at various treatment time points with HO-3867 10μM in the ADOCC mice (Sup. Table-1). A substantial amount of HO-3867 was detected

in ovarian tumor tissues as well as ADOCCs using EPR and LCMS, suggesting that oral supplementation of HO-3867 reached the targeted tumor site. Animals treated with HO-3867 did not show any signs of weight loss or decreased dietary consumption compared to significant decreases in both measures for mice treated with CP (Sup. Fig. S3C. HO-3867 also demonstrated minimal nephrotoxicity compared to CP (Sup. Fig. S4A). The H&E staining showed that the HO-3867 selectively induces necrosis in tumors (Sup. Fig. S4B). Our results suggest that HO-3867 has been shown in the orthotopic mouse model setting to be a selectively cytotoxic and safe anti-cancer drug based on the selective cytotoxic in tumors compare than other organs.

HO-3867 inhibits of ovarian tumor metastasis through the inhibition of STAT3

We observed the presence of numerous metastatic tumors at various sites within the peritoneal cavities and livers of the orthotopic ovarian tumor model mice at the time of sacrifice (Sup. Fig. S5A&B). Fig. 5A (top row) and shows metastatic tumor nodules present on the diaphragms, intestinal mesenteries, and livers in untreated mice. Mice treated with 100 ppm of HO-3867 did not show any significant peritoneal metastases when sacrificed at the end of 6 weeks. (Fig.5A, bottom row). We further quantified tumor metastasis using MRI at the 5^{th} week of HO-3867 and CP treatment and observed a 10 fold decrease in metastasis in the HO-3867 and CP treated mice compared to the untreated controls (Fig.5B). Although our previous reports have demonstrated that HO-3867 specifically targets STAT3 and inhibits ovarian tumor growth, this is the first study where we investigate the therapeutic efficacy of HO-3867 using an orthotopic ovarian tumor model with metastasis. We performed IHC, immunofluorescence (IF) and Western blot analysis of tissues obtained from untreated control and treated mice. The expression of VEGF, which is directly regulated by STAT3, also decreases upon treatment (Fig. 5C & Sup. Fig. S5C). Ki67 and Cyclin D1 also decrease after treatment (2-fold decrease with CP and 4-fold decrease with HO-3867) as compared to the untreated controls (Figure 5D, Sup. Fig. S6). The number of TUNEL positive cells and Caspase-3 shows a 5-fold and 6-fold increase, respectively, after treatment with either CP or HO-3867 (Figure 5D). Decreased Cyclin D1, Bcl-2, and pSTAT3 and increased total and cleaved caspase-3 were also noted by Western blot of mice tumor tissues (Sup. Fig. S5C). To directly test the anti-angiogenic activity of HO-3867 *in vivo*, mice were implanted subcutaneously with Matrigel plugs infused with PBS (control) or VEGF. Mice were treated with 100 ppm of HO-3867 immediately after implantation of the plug and once daily for 7 days. VEGF increased the number of vessels detected in Matrigel plugs by >10-fold over that in PBS infused (control) plugs (Figure 5E). HO-3867 was significantly reduced vessel formation and regulating genes (~4 times) as compared to control (Sup.Fig. S7A &B).

Evaluation of downstream effectors of STAT3 in HO-3867 treated ovarian tumors using proteomic array

The human proteome is subject to a wide variety of post translational modifications, thereby resulting in a number of protein alterations in cancer that cannot be predicted by genomic and transcriptomic methods alone. Sup. Fig. S7C displays hierarchical clustering of $\log_2$ transformed median centered protein expression levels as determined by reverse phase protein array of the untreated tumor samples (A1-3) and treated samples (B1-3, C1-3). The

proteins like VEGFR, ECadherin, JNK2, Src, MAPK, STAT3, Akt, BCl2, Cyclin D1, Cyclin D2, CIAP1 and CIAP2 expressed at intermediate level when compared with untreated controls, as indicated by the black and red colors on the heat map. Table 1 shows STAT3 and its major target proteins related to anti-apoptotic, angiogenesis, and cell proliferation processes which are modulated in HO-3867 treated samples as compared with the untreated controls.

Effect of HO-3867 in ex vivo human ovarian tumor ascites and tissues

Having confirmed the anti-tumor effects of HO-3867 on an orthotopic mouse model, we additionally explored the possibility of testing it on ex vivo human ovarian cancer samples. HO-3867 and CP (10μM) were each administered for 24–72 hr. The STAT3 inhibitor significantly suppressed cell survival in A195 cells (Figure 6A, additional ascites cell lines-A352 and A204 in Sup. Fig. S8). Further, we procured ovarian cancer tissues from patients undergoing cytoreductive surgeries. Uniform 300 μm sections of the tumor tissue were treated with either HO-3867 or CP for up to 72 hours at the indicated concentrations (1,5, 10 and 20μM). (Schematic explanation, Sup. Fig. S9). H&E staining of tumor tissues was obtained after tumor samples were sectioned into 300 μm thick sections using a vibratome and placed into media in the presence or absence of the indicated drugs for 72 hrs followed by sub-sectioning into 4μm sections (Fig. 6B). H&E staining for the untreated ovarian cancer tissue without any treatment and post treatment with HO-3867, CP and STATTIC (a commercially available STAT3 inhibitor), followed by sub-sectioning into 4 μm thin paraffin embedded sections. The cell structure and glandular architecture is intact in the untreated controls at 0 hr and at 72 hours. In contrast to this, there was noticeable cell detachment from the extra-cellular matrix and vacuolated atypical nuclei in all treatments conditions (Figure 6C; Sup. Fig. S10 and 11A&B). The HO-3867 treated tissues showed a marked decrease in pSTAT3 and VEGF along with an increased TUNEL and 8-OHdG positive cells post-treatment as compared to the untreated tumor tissue (Figure 6D and Sup. Fig. S12). Additionally, there was a significant decrease in the relative mRNA expression levels for STAT3 (45.5%) and its associated genes VEGF (57.7%), BCl2 (70.9%), Cyclin D1 (64.2%), and Cyclin D2 (77.4%) (Fig. 6E). These results, further suggest that HO-3867 is a potent anti-cancer drug that acts through a STAT3-mediated mechanism.

Discussion

The important findings of this study are: i) pSTAT3 Tyr705 is constitutively expressed in patient ascites, promoting tumor invasion and metastasis, ii) in vivo studies have shown that STAT-3 knockdown reduces tumor growth and metastatic potential, suggests that STAT3 is required for ovarian cancer progression and metastasis iii) the STAT3 inhibitor HO-3867 significantly suppresses ovarian tumor growth and metastasis in an orthotopic tumor model, iii) HO-3867 is effective in patient tissue cultures in which STAT3 is highly expressed.

Ovarian cancer mortality has not significantly decreased during the last 25 years[24]. Among the reasons for this, there has been a poor understanding of ovarian tumor biology, particularly the expression of oncogenic proteins as well as the interactions with the surrounding tumor microenvironment. Some recent studies have recently found that

malignant ascites enhances tumor cell proliferation and migration[7, 25]. The presence of LPA in ascites has been shown to promote tumor cell proliferation and migration [12]. We have found that constitutive STAT3 expression is present in metastatic tumors from our orthotopic mouse as well as in human metastatic ovarian tumor samples. Other groups have recently reported that the STAT3 cascade mediates up-regulation of MMP2 in SKOV-3 and OVCAR-3 cells which thereby contributes to the invasiveness and metastasis of these ovarian cancer cell lines[26, 27]. Our current and previous data strongly suggest that malignant ascites plays a significant role in facilitating ovarian cancer migration/invasion and metastasis through the activation of oncogenes.

Our in vivo studies show that the level of STAT3 expression directly correlates with the extent and severity of the disease, as the mice injected with ascites with higher pSTAT3 Tyr705 expression had widespread metastases and gross physiology. Using established cell lines, STAT3 knockdown ovarian cancer cells showed reduced tumor growth and metastatic potential when transplanted into the orthotopic mouse model. These findings suggest that STAT3 plays a major role in ovarian cancer progression and metastasis. A previous report showed that gene ablation of STAT3 is required for cellular transformation and/or for tumor survival and growth of lymphoid cells by a deregulated tyrosine kinase[28]. Another group has shown, using a similar approach, that STAT3 is required for transformation and growth of skin tumors induced by chemical carcinogens[29]. The findings from new mouse model described in our present study further supports the tumorigenic role of STATs in cancer.

We found that STAT3 (Tyr705) was constitutively activated (yet pSTAT3 (Ser727) was not) in patient ascites and ascites-derived ovarian cancer cells. This is consistent with prior studies that showed that tyrosine phosphorylation is more important than serine phosphorylation in the activation of STAT3[30]. In addition, the elevated levels of IL-6 and TGF-β secreted by the ascites derived cancer cells into the medium; mediate the activation of STAT3 in STAT3 knockdown cells. The persistent STAT3 activation by IL family proteins such as IL-6, 8, and 11 induces tumorigenesis through the affecting epithelial cells[31, 32, 33]. The exact mechanism by which the expression and regulation of STAT3 play a role in ovarian cancer migration/invasion in patient ascites cells remains unclear. Possible mechanisms for the higher STAT3 expression found in ovarian cancer ascites cells may be a) direct interactions with stromal cells, b) stromal cell-produced cytokines, and c) a phosphatase receptor kinase such as S1PR1, a regulator of STAT3 transcription via the JAK/STAT pathway. A recent study has found that S1PR1 is capable of activating STAT3 through JAK2 tyrosine kinase[34]. In addition, we have reported that S1PR1 is highly expressed in hypoxic ovarian cancer cells[35]. Whether STAT3 activity regulates S1PR1 in high-grade ovarian cancer cells via a positive feedback loop remains to be determined.

Small molecule novel STAT3 inhibitors hold promise as effective targeted therapies for various cancers, including ovarian cancer. Although several STAT3 inhibitors suppress tumor growth in preclinical models[36], thus far none are currently used in the standard treatment of any cancer. Potential reasons for the lack of STAT3 inhibitors in the treatment armamentarium for ovarian cancer include the absence of a clinically relevant model to demonstrate their efficacy[37] as well as difficulties in reaching the target organ[17, 38, 39]. Hence, evaluating novel STAT3 inhibitors using a better orthotopic tumor model, which

more closely mimics the clinical presentation of disease and metastatic progression, is essential. The present study found that the STAT3 inhibitor HO-3867 effectively suppressed tumor growth progression and metastasis through the inhibition of STAT3 in both established and primary ovarian cancer cell orthotopic tumor mouse models. Previous evidence indicated that blocking STAT3 signaling with a small molecule inhibits tumor metastasis and prolong survival of tumor bearing mice[40]. In addition to quantifying the bio-availability of HO-3867, we have also confirmed that this novel STAT3 inhibitor preferentially targets tumor tissue compared to normal tissue. Cytotoxic anti-cancer agents are notorious for poor bioavailability, low solubility in aqueous solutions, and low potency[23, 41, 42]. While the naturally-occuring curcumin as well as the synthetic small molecule STAT3 inhibitors have shown cytotoxicity in various cancer cells by blocking STAT3 signaling[17, 39, 43, 44], their clinical implementation has been hindered by relatively low potency and limited cell permeability[41, 42, 45]. In contrast, the oral bioavailability of HO-3867 and selective absorption into tumor tissue represents a substantial advancement in the application of small-molecule STAT3 inhibitors as unique anticancer agents for ovarian cancer.

To provide a more relevant model to replicate human ovarian cancer, we used ex vivo human ovarian cancer tissue cultures to test the therapeutic efficacy of our novel STAT3 inhibitor. The general procedure of ex vivo cytotoxic drug evaluation, undertaken concurrently with phase I trials in vivo, could enable targets for phase II trials to be identified more rapidly[46]. We have shown that ex vivo organotypic short-term culture of tumor represents a simple method by which the STAT3 pathway targeted by HO-3867 can be rapidly studied with respect to the native heterogeneity of the patient's tumor.

Our study has found that constitutive expression of STAT3 in malignant ascites plays a role in ovarian tumor progression and metastasis. The STAT3-selective targeting agent HO-3867 inhibits of tumor growth and promotes apoptosis both *in vivo* and *ex vivo*, suggesting that HO-3867 has promise as a novel agent for the treatment of ovarian cancer.

Material and Methods

Culture of ascites

Fresh ascites were collected from patients undergoing surgery after informed consent and in accordance with the OSU IRB rules. The ascites were cultured in T75 flasks in RPMI medium in a ratio of 20:20 (v/v). The cells were allowed to stick for 24 hours after which the contents of the flask are removed and replaced with fresh RPMI medium. The cells were allowed to grow to a 100% confluency before freezing them in liquid nitrogen for further use and were called as Ascites Derived Ovarian Cancer Cells (ADOCCs). They were named by de-identified patient numbers as provided by the OSUMC as A179, A183, A202, A195, A263, A352 and A204. The ascites were analyzed for the percent composition of cancer cells via flow cytometry and immunocytochemistry using Vimentin and CD14 markers[47, 48].

Cell lines used in the current study

In addition to the primary ADOCCs collected from different ovarian cancer patients and cultured as explained above, we used three immortalized high grade serous ovarian cancer (HGSOC) human cell lines: A2780, SKOV3 and TR127. A2780 is a cisplatin-resistant cell line developed by chronic exposure of the parent cisplatin-sensitive A2780 cell line (ECACC catalogue no. 93112519) to increasing concentrations of cisplatin. SKOV3 is another cell line resistant to tumor necrosis factor and several cytotoxic drugs including diphtheria toxin, cisplatin and doxorubicin. The SKOV3 cell line is also able to grow in soft agar, an indicator of transformation and tumorigenicity, and displays a relatively high colony forming efficiency. In vivo, SKOV3 cells can form moderately well-differentiated adenocarcinoma consistent with primary ovarian cells. The TR127 cell line, kindly gifted by Dr. G. Mor of Yale University, is derived from recurrent, chemotherapy resistant ovarian cancer tissue. The primary reason for using different cell lines was to prove that tumor progression and metastasis patterns vary widely in established versus primary ovarian cancer cell lines isolated from patient ascites cell lines. We also wanted to prove the anti-cancer efficacy of HO-3867 in an orthotopic tumor model using both established and primary ovarian cancer cell lines.

STAT3 knockdown experiments

For downregulation of STAT3 in A2780 cells, a lentiviral system (pGIPZ) with a set of different short hairpin RNAs (shRNA) was used (Thermo Scientific). The resultant STAT3 knockdown cells were called as A2780 Ko cells. A scrambled shRNA was used as a control.

Cell viability by SRB assay

Ascites derived ovarian cancer cells' (ADOCCs) viability was determined by a colorimetric assay using Sulforhodamine B (SRB). SRB binds to protein components of cells that have been fixed to tissue-culture plates by trichloroacetic acid (TCA). SRB is a bright-pink aminoxanthene dye with two sulfonic groups that bind to basic amino-acid residues under mild acidic conditions, and dissociate under basic conditions. As the binding of SRB is stoichiometric, the amount of dye extracted from stained cells is directly proportional to the cell mass. The cancer cells were grown to 80% confluence in 100 mm culture plates, trypsinized, counted and seeded in 96-well plates with an average population of 8,000 cells/well and collected for the cell viability assays every 24, 48 or 72 hours. All experiments were done using six replicates and repeated at least three times.

Development of orthotopic tumor model

Established cell line SKOV3 or TR-127 ($3 \times 10^{*6}$ cells in 100 μL of PBS) were injected into the ovarian bursa of 6-week-old BALB/c nude mice from the National Cancer Institute. In vivo MRI imaging was done periodically to check upon the tumor growth. After sacrifice, the tumors were measured using a Vernier caliper and weighed in order to get tumor weight, mass and volume. In the therapeutic study groups were treated using the HO-3867 compound mixed with the animal feed (Harlan Teklad) at two different levels (50 and 100 ppm). The tumor volume was measured at the 5^{th} week, 35 days after the beginning of HO-3867 treatment, the mice were sacrificed and the tumors were resected. The tumor

tissues were then subjected to immunoblot analysis, TUNEL assays, and histopathology experiments. Some of the tumor tissues were snap frozen in liquid nitrogen and stored at −80°C for the Real time quantitative PCR and western blots.

Ex vivo slice culture—Fresh specimens of human ovarian carcinoma were obtained under an institutional review board approved protocol with the written informed consent of the patients undergoing surgery. Patients were informed about the nature of the experiments related to ex vivo slice cultures and offered the opportunity to participate by consenting to provide residual tissue obtained from surgery for this study including non-tumor tissue. The tissue specimen was rapidly transported to the laboratory on ice, transferred into ice cold RPMI medium. Living ovarian carcinoma slices (300 μM thick) were generated using a vibrating microtome (Vibratome 1500 series, Vibratome, St. Louis, MO) and transferred to tissue culture dishes containing RPMI/ 5x more antibiotic and allowed to equilibrate at 37°C for 2 hrs and allowed to equilibrate 2 hrs[46, 49]. Subsequently, slices were transferred to cell culture dishes containing RPMI medium with or without 10μM dosage for HO-3867 and CP for a 72 hr. In our experiments, we utilized 3–5 slices per condition (0.5 cm × 0.5 cm × 300 μm), and over 72 h period which was within the viability period for the slices. At end of treatment period, tumor slices were formalin fixed and paraffin embedded for histological processing and immunohistochemial analysis.

RNA isolation and Reverse Transcription PCR (RT PCR)

Freshly excised tumor tissues were snap frozen in liquid nitrogen and stored at −80°C in appropriately labelled vials. At the conclusion of the experimental protocol, total RNA was isolated using the RNeasy Mini Kit (Qiagen, Valencia, CA). RNA samples with an optical density A260/A280 ratio between 1.8 and 2.1 were used. RT-PCR was then performed using the Transcriptor First Strand Complementary DNA (cDNA) Synthesis Kit (Roche Applied Science) to synthesis cDNA. RT-PCR was performed with 1mg of RNA template. The reaction was carried out using the Veriti Thermal Cycler (Applied Biosystems, Carlsbad, CA) and random hexamer primers.

Quantitative Real Time PCR (qPCR)

The genes studied for their relative genetic expression patterns are provided in Table 1. LightCycler 480 SYBR Green I Master Mix (Roche Applied Science) was used to analyze 100 ng of cDNA from each experimental condition along with their respective primers (Table I). qRT-PCR was performed using the Light Cycler 480 System (Roche Applied Science). Each sample was normalized to the control gene glyceraldehyde 3-phosphate dehydrogenase (GAPDH.

Evaluate the bio-absorption of DAPs in ovarian cancer cells using EPR—Our previous study showed that cellular uptake of HO-3867 was significantly greater than curcumin[23]. We evaluated the bio absorption of HO-3867 compounds in ovarian cancer cells and normal hOSE cells using EPR, as previously described[14].

Drug accumulation and metabolism using liquid chromatography mass spectrophotometry (LCMS)—Cellular uptake of the curcumin analogue HO-3867 was

analyzed by a liquid chromatography and tandem mass spectrometry (LC-MS/MS) assay. The assay utilizes a Thermo Finnigan TSQ Quantum Ultra triple quadruple mass spectrometer coupled with Dionex LC module, detailed method previously described[14].

Immunohistochemistry

Fresh-frozen tissue embedded in OCT was sectioned at 5 μm and fixed in phosphate-buffered 4% paraformaldehyde and washed in PBS. The number of cells staining positive was counted by a blinded observer in 5 random 40x fields and compared by the use of Student t test. Images were obtained with an Olympus AX70 fluorescence microscope and Spot v2.2.2 (Diagnostic Instruments, Sterling Heights, MI) digital imaging system. Apoptosis was detected in deparaffinized sections of tumor samples by TdT-mediated dUTP nick-end labeling (TUNEL) assay using the in situ cell death detection kit (Roche, Piscataway, NJ). Distribution and intensity of hypoxia were studied using the recommend protocol for hypoxyprobe-1 (HP1-100; Chemicon International).

Invasion Assay

The Matrigel invasion assays were carried out using Matrigel pre-coated inserts (BD Bioscience) following the manufacturer's instructions. 600μl of M200 medium/ RPMI with or without VEGF (20 ng/ml, R&D Systems) was placed in the lower wells. Proliferating A2780 WT as well as A2780 Ko cells (5×10^5 cells/ml) cells were loaded into each of the upper wells and monitored after 24 hours for the migrating cells.

Vascularization of Matrigel™ Plugs *in vivo*—To further characterize anti-angiogenetic properties of HO 3867 *in vivo*, we performed murine Matrigel plug experiments. An unrelated MoAb/PBS was used as a negative control, and VEGF (100ng/mL) as a positive control. Alternatively plugs containing VEGF (100 ng/ml) were implanted. Matrigel was injected subcutaneously into CB17SC *scid*$^{-/-}$ female mice, forming semi-solid plugs. The control group was given a normal diet (no treatment) while the experimental groups were treated using the HO-3867 compounds mixed with the animal feed. On day 7, plugs were excised under anesthesia, fixed in PBS-buffered 10% formalin containing 0.25% glutaraldehyde, and were processed for H & E and Masson's Trichrome staining. Vascular identity of the infiltrating cells was established with CD34 immunostaining. The regions containing the most intense area of neovascularization (“hotspots”) were chosen for analysis. Eight hotspots were identified for each Matrigel or tumor section. The ImagePro Plus analysis system was used to quantify the percentage of area occupied by the vessel-like structures in each field. The mean ± SE from each group were compared. The negative control was obtained

Statistical Analysis

Data are presented as mean±1 standard deviation. To determine statistical significance among groups analysis of variance (ANOVA) was first performed. If ANOVA was statistically significant, the student's t-test was then performed to compare sub-groups, p-value <0.05 was considered as statistically significant.

Supplementary Material

Refer to Web version on PubMed Central for supplementary material.

Acknowledgements

We are very thankful to Dr. John Hays for his willingness to pre-review this manuscript and provide valuable comments and suggestions. We would like to thank Dr. Vinay Puduvalli and his lab members (including Jihong Xu) for providing access to their vibrating microtome. We extend additional thanks to Dr. Mitch Phelps and Dr. Yonghua Ling of the Pharmacoanalytical Shared Resource (PhASR), for LCMS analysis of drug bio-absorption and metabolism. The authors are also thankful to the undergraduate students Ross Wanner, Riley Maria, Roman Zingarelli and Jack Fowler for the cell culture and basic assay help. This work was funded by Ovarian Cancer Research Fund (OCRF), NCI RO1-CA176078 grant and Drug Development Institute pilot grant (K.S. and D.E.C), and OSU CCC Internal grant to D.E.C.

References

1. Siegel RL, Miller KD, Jemal A. Cancer statistics, 2015. CA: a cancer journal for clinicians. 2015; 65(1):5–29. [PubMed: 25559415]
2. Coleman RL, Monk BJ, Sood AK, Herzog TJ. Latest research and treatment of advanced-stage epithelial ovarian cancer. Nature reviews Clinical oncology. 2013; 10(4):211–224.
3. Lengyel E. Ovarian cancer development and metastasis. The American journal of pathology. 2010; 177(3):1053–1064. [PubMed: 20651229]
4. Naora H, Montell DJ. Ovarian cancer metastasis: integrating insights from disparate model organisms. Nature reviews Cancer. 2005; 5(5):355–366. [PubMed: 15864277]
5. Pradeep S, Kim SW, Wu SY, Nishimura M, Chaluvally-Raghavan P, Miyake T, et al. Hematogenous metastasis of ovarian cancer: rethinking mode of spread. Cancer cell. 2014; 26(1):77–91. [PubMed: 25026212]
6. Ahmed N, Stenvers KL. Getting to know ovarian cancer ascites: opportunities for targeted therapy-based translational research. Frontiers in oncology. 2013; 3:256. [PubMed: 24093089]
7. Kipps E, Tan DS, Kaye SB. Meeting the challenge of ascites in ovarian cancer: new avenues for therapy and research. Nature reviews Cancer. 2013; 13(4):273–282. [PubMed: 23426401]
8. Latifi A, Luwor RB, Bilandzic M, Nazaretian S, Stenvers K, Pyman J, et al. Isolation and characterization of tumor cells from the ascites of ovarian cancer patients: molecular phenotype of chemoresistant ovarian tumors. PloS one. 2012; 7(10):e46858. [PubMed: 23056490]
9. Selvendiran K, Bratasz A, Kuppusamy ML, Tazi MF, Rivera BK, Kuppusamy P. Hypoxia induces chemoresistance in ovarian cancer cells by activation of signal transducer and activator of transcription 3. International journal of cancer Journal international du cancer. 2009; 125(9):2198–2204. [PubMed: 19623660]
10. Pradeep S, Huang J, Mora EM, Nick AM, Cho MS, Wu SY, et al. Erythropoietin Stimulates Tumor Growth via EphB4. Cancer cell. 2015
11. Selvendiran K, Tong L, Bratasz A, Kuppusamy ML, Ahmed S, Ravi Y, et al. Anticancer efficacy of a difluorodiarylidenyl piperidone (HO-3867) in human ovarian cancer cells and tumor xenografts. Molecular cancer therapeutics. 2010; 9(5):1169–1179. [PubMed: 20442315]
12. Selvendiran K, Ahmed S, Dayton A, Ravi Y, Kuppusamy ML, Bratasz A, et al. HO-3867, a synthetic compound, inhibits the migration and invasion of ovarian carcinoma cells through downregulation of fatty acid synthase and focal adhesion kinase. Molecular cancer research : MCR. 2010; 8(9):1188–1197. [PubMed: 20713491]
13. Tierney BJ, McCann GA, Naidu S, Rath KS, Saini U, Wanner R, et al. Aberrantly activated pSTAT3-Ser727 in human endometrial cancer is suppressed by HO-3867, a novel STAT3 inhibitor. Gynecologic oncology. 2014; 135(1):133–141. [PubMed: 25038288]
14. Rath KS, Naidu SK, Lata P, Bid HK, Rivera BK, McCann GA, et al. HO-3867, a safe STAT3 inhibitor, is selectively cytotoxic to ovarian cancer. Cancer research. 2014; 74(8):2316–2327. [PubMed: 24590057]

15. Kalai T, Kuppusamy ML, Balog M, Selvendiran K, Rivera BK, Kuppusamy P, et al. Synthesis of N-substituted 3,5-bis(arylidene)-4-piperidones with high antitumor and antioxidant activity. Journal of medicinal chemistry. 2011; 54(15):5414–5421. [PubMed: 21702507]
16. Tierney BJ, McCann GA, Cohn DE, Eisenhauer E, Sudhakar M, Kuppusamy P, et al. HO-3867, a STAT3 inhibitor induces apoptosis by inactivation of STAT3 activity in BRCA1-mutated ovarian cancer cells. Cancer biology & therapy. 2012; 13(9):766–775. [PubMed: 22801507]
17. Kim D, Lee IH, Kim S, Choi M, Kim H, Ahn S, et al. A specific STAT3-binding peptide exerts antiproliferative effects and antitumor activity by inhibiting STAT3 phosphorylation and signaling. Cancer research. 2014; 74(8):2144–2151. [PubMed: 24576829]
18. Kroon P, Berry PA, Stower MJ, Rodrigues G, Mann VM, Simms M, et al. JAK-STAT blockade inhibits tumor initiation and clonogenic recovery of prostate cancer stem-like cells. Cancer research. 2013; 73(16):5288–5298. [PubMed: 23824741]
19. Zhang X, Yue P, Page BD, Li T, Zhao W, Namanja AT, et al. Orally bioavailable small-molecule inhibitor of transcription factor Stat3 regresses human breast and lung cancer xenografts. Proceedings of the National Academy of Sciences of the United States of America. 2012; 109(24): 9623–9628. [PubMed: 22623533]
20. Mace TA, Ameen Z, Collins A, Wojcik S, Mair M, Young GS, et al. Pancreatic cancer-associated stellate cells promote differentiation of myeloid-derived suppressor cells in a STAT3-dependent manner. Cancer research. 2013; 73(10):3007–3018. [PubMed: 23514705]
21. Selvendiran K, Koga H, Ueno T, Yoshida T, Maeyama M, Torimura T, et al. Luteolin promotes degradation in signal transducer and activator of transcription 3 in human hepatoma cells: an implication for the antitumor potential of flavonoids. Cancer research. 2006; 66(9):4826–4834. [PubMed: 16651438]
22. Huang F, Tong X, Fu L, Zhang R. Knockdown of STAT3 by shRNA inhibits the growth of CAOV3 ovarian cancer cell line in vitro and in vivo. Acta biochimica et biophysica Sinica. 2008; 40(6): 519–525. [PubMed: 18535750]
23. Dayton A, Selvendiran K, Kuppusamy ML, Rivera BK, Meduru S, Kalai T, et al. Cellular uptake, retention and bioabsorption of HO-3867, a fluorinated curcumin analog with potential antitumor properties. Cancer biology & therapy. 2010; 10(10):1027–1032. [PubMed: 20798598]
24. Goff B. Measuring ovarian cancer care: why are we still failing? Gynecologic oncology. 2015; 136(1):1–2. [PubMed: 25554011]
25. Matte I, Lane D, Bachvarov D, Rancourt C, Piche A. Role of malignant ascites on human mesothelial cells and their gene expression profiles. BMC cancer. 2014; 14:288. [PubMed: 24761768]
26. Seo JM, Park S, Kim JH. Leukotriene B4 receptor-2 promotes invasiveness and metastasis of ovarian cancer cells through signal transducer and activator of transcription 3 (STAT3)-dependent up-regulation of matrix metalloproteinase 2. The Journal of biological chemistry. 2012; 287(17): 13840–13849. [PubMed: 22396544]
27. Gritsina G, Xiao F, O'Brien SW, Gabbasov R, Maglaty MA, Xu RH, et al. Targeted Blockade of JAK/STAT3 Signaling Inhibits Ovarian Carcinoma Growth. Molecular cancer therapeutics. 2015
28. Chiarle R, Simmons WJ, Cai H, Dhall G, Zamo A, Raz R, et al. Stat3 is required for ALK-mediated lymphomagenesis and provides a possible therapeutic target. Nature medicine. 2005; 11(6):623–629.
29. Pedranzini L, Leitch A, Bromberg J. Stat3 is required for the development of skin cancer. The Journal of clinical investigation. 2004; 114(5):619–622. [PubMed: 15343379]
30. Lee MY, Joung YH, Lim EJ, Park JH, Ye SK, Park T, et al. Phosphorylation and activation of STAT proteins by hypoxia in breast cancer cells. Breast. 2006; 15(2):187–195. [PubMed: 16084091]
31. Yu H, Lee H, Herrmann A, Buettner R, Jove R. Revisiting STAT3 signalling in cancer: new and unexpected biological functions. Nature reviews Cancer. 2014; 14(11):736–746. [PubMed: 25342631]
32. Putoczki T, Ernst M. More than a sidekick: the IL-6 family cytokine IL-11 links inflammation to cancer. Journal of leukocyte biology. 2010; 88(6):1109–1117. [PubMed: 20610798]

33. Ernst M, Najdovska M, Grail D, Lundgren-May T, Buchert M, Tye H, et al. STAT3 and STAT1 mediate IL-11-dependent and inflammation-associated gastric tumorigenesis in gp130 receptor mutant mice. The Journal of clinical investigation. 2008; 118(5):1727–1738. [PubMed: 18431520]
34. Lee H, Deng J, Kujawski M, Yang C, Liu Y, Herrmann A, et al. STAT3-induced S1PR1 expression is crucial for persistent STAT3 activation in tumors. Nature medicine. 2010; 16(12):1421–1428.
35. McCann GA, Naidu S, Rath KS, Bid HK, Tierney BJ, Suarez A, et al. Targeting constitutively-activated STAT3 in hypoxic ovarian cancer, using a novel STAT3 inhibitor. Oncoscience. 2014; 1(3):216–228. [PubMed: 25594014]
36. Darnell JE. Validating Stat3 in cancer therapy. Nature medicine. 2005; 11(6):595–596.
37. Venkatesh S, Lipper RA. Role of the development scientist in compound lead selection and optimization. Journal of pharmaceutical sciences. 2000; 89(2):145–154. [PubMed: 10688744]
38. Siddiquee K, Zhang S, Guida WC, Blaskovich MA, Greedy B, Lawrence HR, et al. Selective chemical probe inhibitor of Stat3, identified through structure-based virtual screening, induces antitumor activity. Proceedings of the National Academy of Sciences of the United States of America. 2007; 104(18):7391–7396. [PubMed: 17463090]
39. Wen W, Liang W, Wu J, Kowolik CM, Buettner R, Scuto A, et al. Targeting JAK1/STAT3 signaling suppresses tumor progression and metastasis in a peritoneal model of human ovarian cancer. Molecular cancer therapeutics. 2014
40. Kortylewski M, Kujawski M, Wang T, Wei S, Zhang S, Pilon-Thomas S, et al. Inhibiting Stat3 signaling in the hematopoietic system elicits multicomponent antitumor immunity. Nature medicine. 2005; 11(12):1314–1321.
41. Anand P, Kunnumakkara AB, Newman RA, Aggarwal BB. Bioavailability of curcumin: problems and promises. Molecular pharmaceutics. 2007; 4(6):807–818. [PubMed: 17999464]
42. Cheng X, Rasque P, Vatter S, Merz KH, Eisenbrand G. Synthesis and cytotoxicity of novel indirubin-5-carboxamides. Bioorganic & medicinal chemistry. 2010; 18(12):4509–4515. [PubMed: 20488718]
43. Hsu HS, Huang PI, Chang YL, Tzao C, Chen YW, Shih HC, et al. Cucurbitacin I inhibits tumorigenic ability and enhances radiochemosensitivity in nonsmall cell lung cancer-derived CD133-positive cells. Cancer. 2011; 117(13):2970–2985. [PubMed: 21225866]
44. Bill MA, Fuchs JR, Li C, Yui J, Bakan C, Benson DM Jr, et al. The small molecule curcumin analog FLLL32 induces apoptosis in melanoma cells via STAT3 inhibition and retains the cellular response to cytokines with anti-tumor activity. Molecular cancer. 2010; 9:165. [PubMed: 20576164]
45. Greten FR, Karin M. Peering into the aftermath: JAKi rips STAT3 in cancer. Nature medicine. 2010; 16(10):1085–1087.
46. Vaira V, Fedele G, Pyne S, Fasoli E, Zadra G, Bailey D, et al. Preclinical model of organotypic culture for pharmacodynamic profiling of human tumors. Proceedings of the National Academy of Sciences of the United States of America. 2010; 107(18):8352–8356. [PubMed: 20404174]
47. Bolyard C, Yoo JY, Wang PY, Saini U, Rath KS, Cripe TP, et al. Doxorubicin synergizes with 34.5ENVE to enhance antitumor efficacy against metastatic ovarian cancer. Clinical cancer research : an official journal of the American Association for Cancer Research. 2014; 20(24): 6479–6494. [PubMed: 25294909]
48. Yoo JY, Hurwitz BS, Bolyard C, Yu JG, Zhang J, Selvendiran K, et al. Bortezomib-induced unfolded protein response increases oncolytic HSV-1 replication resulting in synergistic antitumor effects. Clinical cancer research : an official journal of the American Association for Cancer Research. 2014; 20(14):3787–3798. [PubMed: 24815720]
49. Pirnia F, Frese S, Gloor B, Hotz MA, Luethi A, Gugger M, et al. Ex vivo assessment of chemotherapy-induced apoptosis and associated molecular changes in patient tumor samples. Anticancer research. 2006; 26(3A):1765–1772. [PubMed: 16827105]

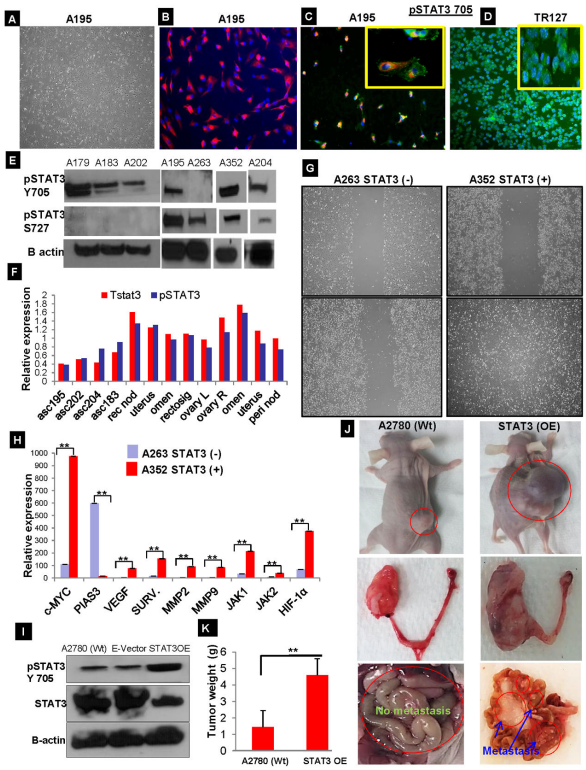

Fig. 1.

Isolation and characterization of ascites derived cancer cells. (**A**) Ascites fluid was collected from consented ovarian cancer patients and cultured on a T-75 flask. At the end of 18 hours, the ascites-derived cancer cells (ADOCCs) were attached to the bottom of the plate (4X magnification). (**B**) The ADOCCs (A195) were characterized for their epithelial origin using the epithelial-exclusive marker EpCam, which appears red in the picture (10X magnification). (**C**) ADOCCs (A195) stained for pSTAT3 705 (green) showed intracytoplasmic accumulation in 98–99% of the cell population (10X magnification). The inset shows a close-up of the cells (20X magnification). (**D**) pSTAT3 705 in TR127 cells (ascites derived immortalized cell line) displaying nuclear accumulation of pSTAT3. (**E**) Western blot of STAT3 proteins from different ADOCCs collected from different patients. A263 lacked pSTAT3 705 expression and A352 had a higher STAT3 expression compared to samples from other subjects; these two samples were used for subsequent experiments. (**F**) Ascites fluids, samples from primary ovarian tumor and metastatic sites in different patients were collected; protein extracted from these samples was subjected to pSTAT3 and total STAT3 ELISA assays. Primary ovarian tumor and the metastasized sites had shown the highest levels of pSTAT3 Tyr705 expression. (**G**) The cells with higher (A352) and lower (A263) STAT3 expression were subjected to wound healing assays in order to understand the correlation between STAT3 expression level and migration capability. The top panels show the plates at 0 hr after scratch and the bottom panels show the migration pattern after 24 hours. The cells over-expressing STAT3 (A352) migrate and close the gap within the first 24 hours (bottom right) while the cells with lower STAT3 expression (A263) do not (bottom left). (**H**) RNA was extracted from the higher STAT3 (A352) and lower STAT3 (A263) expression ascites and subjected to real time PCR after reverse transcription. As is evident

from the figure, the STAT3-associated genes were expressed at higher levels in the cells expressing higher levels of STAT3 (A352). The experiment was repeated 3 times with 4 replicates per sample. ** over the bars in the graph indicates a p value ≤ 0.005 (**I**) In order to create STAT3 overexpression cells, A2780 cells were transfected with a vector harboring STAT3 gene (STAT3 OE) or with the empty vector backbone (E-Vector) for control. The OE was confirmed using Western blot. (**J**) The panel shows orthotopic mice injected with A2780 Wt and STAT3 overexpression (STAT3 OE) cells. Each mouse developed a big tumor and ascites within 2 weeks of injection; peritoneal, hepatic, and intestinal metastases were observed. The tumor weight was significantly higher in STAT3 OE transplanted mice compare with A2780 (Wt) type tumor ((p value ≤ 0.005).

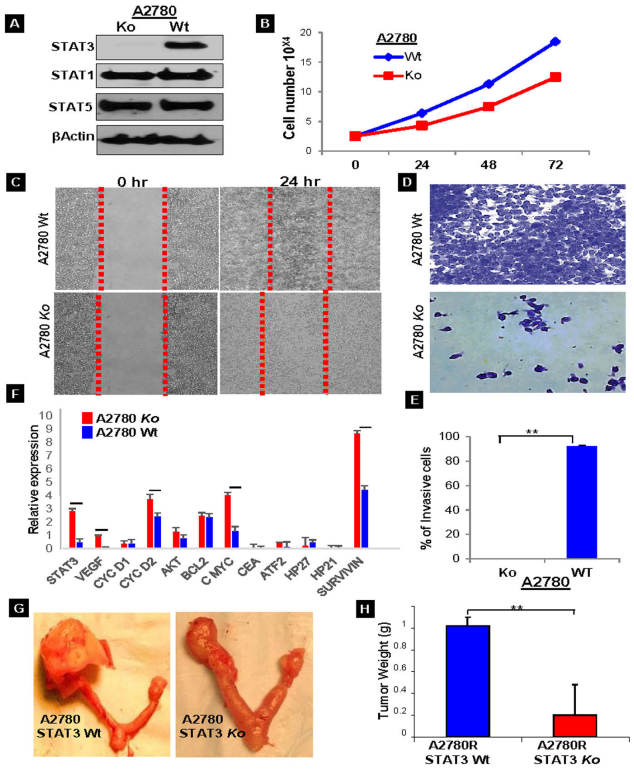

Fig. 2.

STAT3 knockdown (*Ko*) characterization: (**A**) A2780 cells were transfected with STAT3 shRNA and the knockdown was confirmed with Western Blot for the expression of STAT1, STAT3 and STAT5. (**B**) Cell viability assays were performed on the A2780 Wt and *Ko* cells using SRB reagent. The graph displays the cell numbers versus time. (**C**) Scratch assays were performed on the Wt and *Ko* cells to analyze the migration capability of the cells. (**D**&**E**) Invasion assays for Wt and *Ko* cells was performed (n=3) using matrigel precoated inserts and the number of cells invading onto the opposite side of the membrane were counted and plotted as a graph (p value ≤ 0.005). (**F**) Real time quantitative PCR was performed for the relative mRNA expression of STAT3 and associated genes in Wt and *Ko* cells. The values were calculated using the 2(-Delta Delta C(T)) method and were normalized to the housekeeping gene GAPDH. Each experiment was repeated thrice and each sample had 4 replicates. The horizontal line over the bars indicates that the results are significant with a p value ≤ 0.005. (**G**&**H**) the Wt and *Ko* cells were injected into nude mice (n=3) to evaluate for tumor growth and metastasis in vivo. The mice injected with Wt cells had a large ovarian tumor as compared to the mice injected with *Ko* cells.

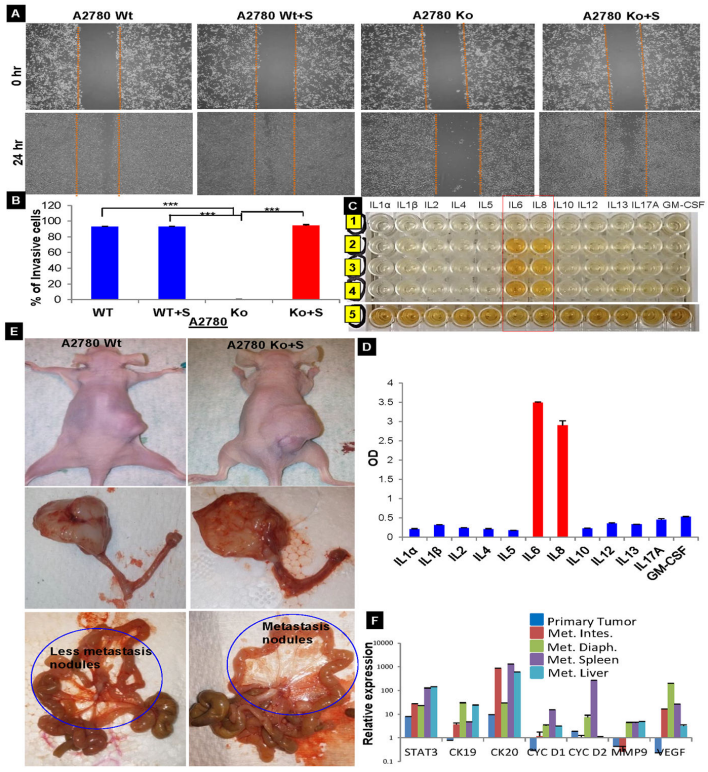

Fig. 3.

Effect of ascites conditioned medium on migration, invasion and tumor burden (**A**) The A2780 Wt and *Ko* cells were treated with conditioned medium collected from ascites in culture. Scratch assay showed that the addition of conditioned medium made up for the absence of STAT3 and restored the vigorous migration and (**B**) invasion in the *Ko* cells (n=3; *** indicate a p value ≤ 0.0005). (**C**&**D**) Multi analyze cytokine ELISA array for simultaneous detection of 12 cytokines (n=3). (**E**) A2780 Wt and Ko cells treated with supernatant injected into the ovarian bursa of nude mice and monitored for 6 weeks post injection. The tumor size and mesenteric metastases were comparable in both cases. (**F**) Relative expression levels of mRNA of the harvested tissues (primary ovarian cancer tissue as well as the metastasized sites) revealed higher expression of STAT3, CK19, CK20, cyc D1, cyc D2, MMP9, and VEGF as compared to the primary ovarian cancer tissue. Each experiment repeated 43 times with 3 replicates per sample.

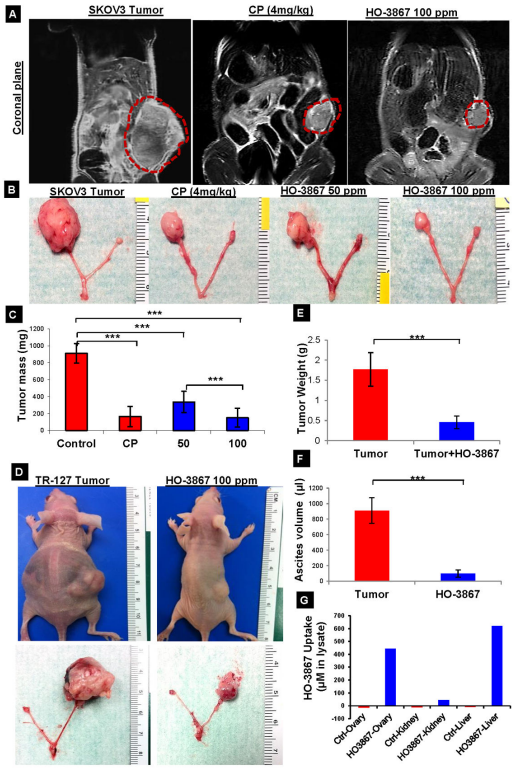

Fig. 4.

HO-3867 mediated inhibition of orthotopic ovarian tumor growth and bioavailability of HO-3867 in mice (n=3). (**A**) In vivo MRI imaging after 4 weeks of control (untreated), HO-3867, or cisplatin. (**B**) Terminal gross pathology images of ovarian tumor in HO-3867 (50 and 100 ppm) and cisplatin (4 mg/kg weekly twice) after 4 weeks of treatment demonstrate reduced tumor volume (n=8) (**C**) Tumor mass after treatment with 100 ppm of HO-3867 was significantly reduced in comparison to untreated for cisplatin-treated tumors (4mg/kg) ($p \leq 0.0005$). (**D**) TR-127 cells were transplanted into the ovarian bursa of nude mice to evaluate the efficacy of HO-3867- dorsal view of untreated control and 100 ppm HO-3867 mice treated for 4weeks. (**E**) Significant ($p<0.0005$, n=5) reductions in tumor weight and (**F**) ascites volume were observed after treatment with HO-3867. (**G**) Bioavailability of HO-3867 was determined using EPR in orthotopic ovarian tumor bearing mice after 24 hours of treatment with 100 ppm of HO-3867, demonstrates significant bio-absorption in ovarian tumor and liver tissues (n=6).

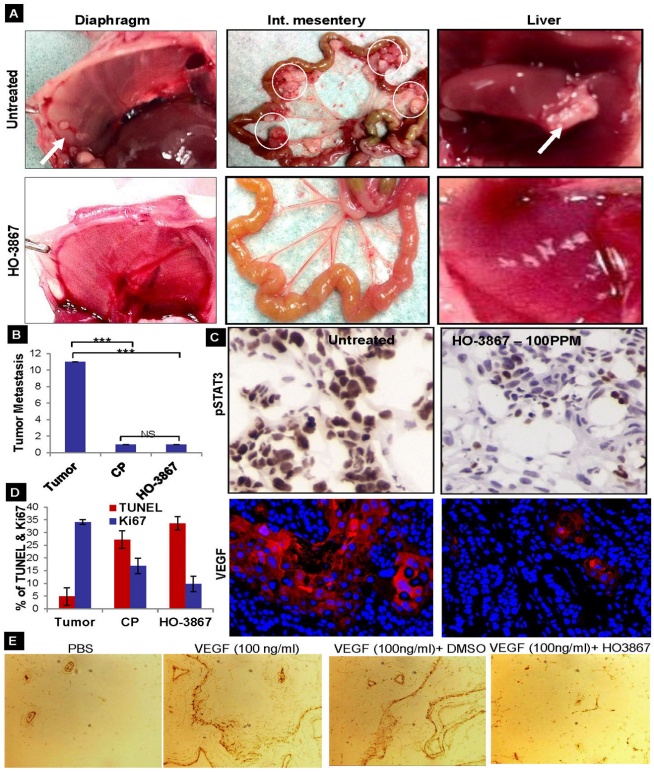

Fig. 5.

Inhibition of metastasis by HO-3867 treatment. (**A**) HO-3867 suppresses the frequency of tumor metastasis as observed on gross pathology of diaphragm, intestinal mesentery, and liver (**B**) Quantification of tumor metastases using MRI at the 5th week of HO-3867 and cisplatin treatments ($p < 0.0005$; n=5) (**C**) IHC/IF analysis of HO-3867 treatment showed reduced levels of pSTAT3 and VEGF staining in orthotopic ovarian tumor tissues. The pSTAT3 IHC images were taken at a higher magnification of 40X to pinpoint the nuclear or cytoplasmic localization. VEGF stained images were shown at higher magnification (40X) to visualize the scattered areas of less positively stained areas in treated tumors. (**D**) Quantification of cell proliferation and apoptosis ($p<0.05$; n=3). (**E**) In vivo Matrigel assay; sections were stained for CD34. The numbers of CD34-positive vessels per high power field were counted for each experimental condition ($p<0.005$; n=3).

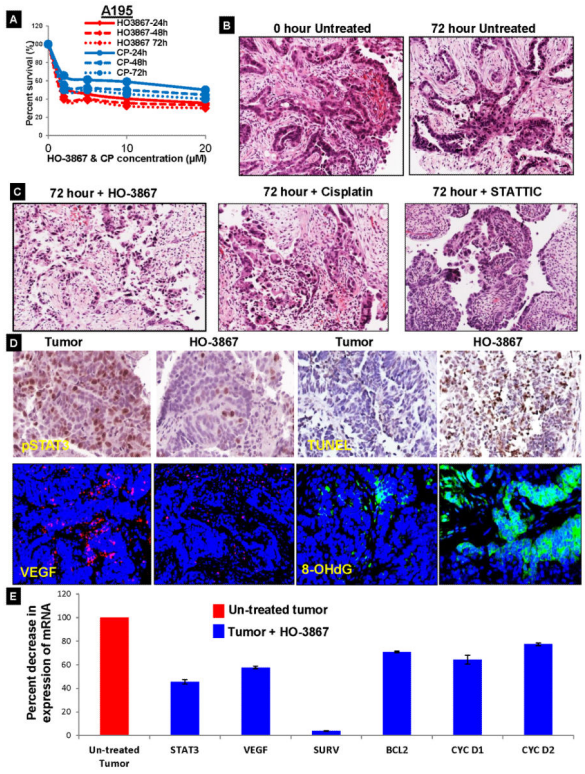

Fig. 6.

Effect of HO-3867 in ex vivo human ovarian tumor tissues. **(A)** Percent survival of A195 cells treated with variable concentrations of HO-3867 and cisplatin at multiple time intervals (n=3). The time points indicate the time after drug exposure before cells counting. (**B**&**C**) H&E staining of human ovarian tumor tissue showing the tissue morphology in untreated controls or treatment with HO-3867 10μM, cisplatin 10 mg/ml, or STATTIC 25μM treatments (n=3). Notably, tissue architecture was intact for 72 hours in the untreated ground, but there was dramatic loss and necrosis of tumor cells in treated group. These changes were more prominent in HO-3867 treated tumor slices ($p \leq 0.0005$; NS-non significant). (**D**) pSTAT3 and VEGF were decreased and increased TUNEL and 8-OHdG were increased on staining representative human tissues treated with HO-3867 10 μM treatment 72 hr (40x magnification). (**E**) Percent decrease in mRNA expression of STAT3 and its target genes as evaluated by RT-PCR after no treatment or administration of HO-3867 10μM. Each experiment was repeated thrice and each sample had 4 replicates.

Table 1

Major STAT3 target proteins which are modulated in HO-3867 in treated samples and untreated controls as using reverse phase protein array.

Target Protein	P value	Mean Untreated	Mean Treated	Difference	SE of difference	% Change From baseline
Down regulated by treatment with HO-3867						
*MEK1-R-V	0.00471375	1.16321	0.748007	0.415205	0.0729797	**−35.6946**
*EGFR-R-V	0.00473408	1.69287	1.01438	0.678492	0.119399	**−40.0793**
*PI3K-p110-alpha-R-C	0.00715288	1.44178	1.34066	0.101112	0.0199609	**−7.01355**
Notch1-R-V	0.0296148	3.47793	2.51749	0.960438	0.290037	**−27.6153**
p27-R-V	0.0311367	0.754569	0.633443	0.121127	0.0371772	**−16.0523**
EGFR_pY1068-R-C	0.0379336	0.805608	0.505846	0.299762	0.0982006	**−37.2094**
HER2_pY1248-R-C	0.0440545	0.524731	0.329672	0.195059	0.0672283	**−37.1731**
mTOR_pS2448-R-C	0.0744822	1.4906	1.36394	0.126657	0.052808	**−8.49725**
JNK2-R-C	0.0811857	1.016	0.857035	0.158966	0.0685359	**−15.6462**
Src_pY527-R-V	0.105242	6.20754	5.40947	0.798067	0.382485	**−12.8565**
VEGFR2-R-V	0.195034	5.78812	5.00227	0.785845	0.505526	**−13.5769**
MEK1_pS217_S221-R-V	0.609548	0.68778	0.665064	0.0227166	0.0410591	**−3.3028**
Up regulated by treatment with HO-3867						
*p53-R-E	0.0174394	0.187616	0.258572	−0.0709555	0.0181616	**37.8198**
p27_pT157-R-C	0.0209659	0.541656	0.621135	−0.0794791	0.0215223	**14.67334**
JNK_pT183_pY185-R-V	0.043645	0.652717	0.732696	−0.0799792	0.0274771	**12.25324**
cIAP-R-C	0.0449899	2.38703	2.67331	−0.286276	0.0993839	**11.99315**
Bak-R-C	0.0599533	1.68703	1.84631	−0.159283	0.0612271	**9.441444**
p27_pT198-R-V	0.0967743	1.28654	1.40279	−0.116257	0.0537964	**9.035864**